The reactivity of lattice nitrogen within the Ni_2Mo_3N and $NiCoMo_3N$ phases

Samia AlSobhi,[a] Nicolas Bion[b], Justin S. J. Hargreaves,[c] Andrew L. Hector,[a] Said Laassiri,[c] William Levason,[a] Andrew W. Lodge,[a] Andrew R. McFarlane[c] and Clemens Ritter[d]

[a] School of Chemistry, University of Southampton, Southampton SO17 1BJ, UK
[b]University of Poitiers, CNRS UMR 7285 Institut de Chimie des Milieux et Matériaux de Poitiers (IC2MP), 4 rue Michel Brunet, TSA 51106, 86073 Poitiers Cedex 9, France
[c] School of Chemistry, University of Glasgow, Glasgow G12 8QQ, UK
[d] Institut Laue-Langevin, Boîte Postale 156, 38042 Grenoble Cedex 9, France

In this study, the reactivity of bulk lattice nitrogen within the filled β-Mn structured Ni_2Mo_3N phase has been investigated by application of powder neutron diffraction and heterolytic nitrogen isotopic exchange measurements. In contrast to Co_3Mo_3N, despite the similarity in the N immediate local environment comprising NMo_6 octahedra, its reactivity is found to be limited and this lower reactivity was maintained upon the introduction of a significant proportion of cobalt to yield its filled β-Mn structured $CoNiMo_3N$ quaternary nitride counterpart.

Key words: Nitride, catalysis, ammonia synthesis, neutron diffraction, isotopic exchange.

Introduction

The reactivity of the lattice nitrogen within metal nitrides is of interest for the development of catalysts and chemical looping reagents [1]. In a series of publications on chemical looping, Pfromm and co-workers have detailed the production of sustainable fossil free ammonia applying solar based routes [2–8]. The approach adopted involves the hydrolysis of an intermediate nitride which is regenerated from N_2 at very high temperatures achieved *via* application of concentrated solar radiation. The intermediate nitrides investigated have included those of molybdenum [7], chromium [2], magnesium [5] and manganese [7,8] with studies documenting the role of iconicity [5] and the application of promoters [8]. Sustainable ammonia production *via* a cycle which involves the hydrolysis of lithium nitride and a molten salt electrolysis step which can performed using sustainably derived electricity has recently been reported by Nørskov and co-workers [9]. The liberation of ammonia accomplished *via* the hydration of magnesium nitride has also been of interest for organic synthesis, although extreme caution is required in its application [10–12]. A number of other studies have investigated the liberation of ammonia via the hydrogenation of metal nitrides and such studies have included Cu_3N [13], Ni_3N [13] and Ta_3N_5 [13,14] in addition to cobalt [15], iron [15], rhenium [15] and manganese [16] nitrides. In the case of Ta_3N_5, on the basis of computational modelling studies, the favorable effect of cobalt upon the liberation of ammonia was ascribed to enhanced hydrogen activation and lowered nitrogen vacancy formation energy [17].

In terms of catalytic processes, there is interest in the possibility that Co_3Mo_3N acts as an effective ammonia synthesis catalyst *via* the Mars-van Krevelen mechanism in which ammonia production involves hydrogenation of lattice nitrogen generating transient vacancies which are replenished from gas-phase N_2. In this context, it is noteworthy that Co_3Mo_3N can be reduced by H_2 to form the Co_6Mo_6N

phase in which the lattice N has relocated from the 16*c* Wyckoff site to the 8*a* site [18,19]. Some liberation of ammonia occurs in this stoichiometric process [18] and regeneration of the original Co_3Mo_3N phase is possible by application of a N_2/H_2 reactant mixture [19] or, at higher temperature, N_2 alone [20]. This observation demonstrates both that the reactivity of the lattice N in Co_3Mo_3N can be of importance in its application as an ammonia synthesis catalyst and that Co_3Mo_3N is a potential reversible N discharge reagent which could be of interest in the development of a chemical looping system. Further evidence for the reactivity of lattice N in the Co_3Mo_3N system comes from the observation that it is active for $^{15}N_2$ exchange, with significant levels of N exchange occurring at 600 °C dependent upon pre-treatment [21]. In this context, computational modelling has indicated that significant N vacancy concentrations exist on the (111) surface at ammonia synthesis reaction temperatures [22]. Extended studies have probed the reaction mechanism [23], raising the tantalizing prospect of an associative N_2 activation pathway for ammonia synthesis which could be relevant for the development of low temperature catalysts [24]. Interestingly, studies of the isostructural Fe_3Mo_3N system have demonstrated that its lattice N is much less reactive than that of its Co counterpart [25]. In studies of the $Co_{3-x}Fe_xMo_3N$ quaternary systems, Co rich phases seem to perform in a similar manner to Co_3Mo_3N whereas iron rich phases are similar to Fe_3Mo_3N [26]. The overall difference in lattice N reactivity between the two pure phases is perhaps somewhat surprising in view of the similarity of N local environment, in which N is coordinated in a distorted octahedral arrangement of six Mo atoms. This suggests the origin of the difference to more subtly involve the Fe and Co component through a secondary effect, possibly an inter-relation between the H_2 surface activation and the lattice N activity, since the differences do not lie within the first coordination shell of the lattice N.

Despite the similarity in local N coordination environment, the filled β-Mn structured Ni_2Mo_3N phase has lower reactivity than Co_3Mo_3N [27]. Co_2Mo_3N was also recently shown not to be reduced under H_2, in contrast to Co_3Mo_3N [28]. In order to obtain enhanced understanding of the origin of lattice N reactivity, to develop heterogeneous catalysts and electrocatalysts of enhanced performance [29–32] along with novel nitrogen looping reagents, it is necessary to expand the range of nitride systems investigated and to determine key differences associated with lattice N reactivity. Herein we examine the lattice N activity of Ni_2Mo_3N and $NiCoMo_3N$ using *in situ* neutron diffraction and isotopic exchange studies.

Experimental

Ni_2Mo_3N and $NiCoMo_3N$ were produced using a modified Pechini route as described previously [27], except that samples were fired in ammonia at a higher temperature (900 °C for 12 h) to remove an impurity phase that was observed at lower synthesis temperatures.

In a typical catalytic activity test, 0.3 g of the nitride catalyst was placed in a silica reactor tube and was pre-treated for 2 h at 700 °C under a 75 vol.% H_2 in N_2 (BOC, 99.98%) gas mixture. The reaction was then performed under the same 75% H_2/N_2 at a total gas feed of 60 NTP ml min^{-1}. Ammonia production was determined by measurement of the decrease in conductivity of a 200 ml 0.0018 M H_2SO_4 solution through which the reactor effluent stream flowed.

Nitrogen Isotopic exchange experiments were performed in an apparatus described elsewhere [27]. In summary, a U-form reactor was placed in a closed recycle system with one side connected to a mass spectrometer (Pfeiffer Vacuum, QMS 200) for monitoring the gas phase composition. Temperature-

programmed isotopic exchange was conducted on 100 mg of each of the catalysts. Prior to the isotopic exchange experiment, samples were subjected to an *in situ* 75% H_2/N_2 activation step at 700 °C for 1 h and a N_2 purge for 30 min. The samples were then cooled under N_2 at 400°C and degassed for 30 min. The study of isotopic nitrogen exchange was performed using $^{15}N_2$ (98% + purity, supplied by Cambridge Isotope Laboratories, Inc.). The mass-to-charge ratios of 28, 29 and 30 m/z were monitored as a function of time to follow the exchange process.

Powder neutron diffraction (PND) measurements were carried out on D20 at the Institut Laue-Langevin using the 90° take-off angle mode and with a neutron wavelength of 1.5436 Å. Samples with mass around 200 mg were loaded into a 10 mm O/D, 8 mm I/D silica tube which was flushed with 75% H_2 (30 cm^3 min^{-1}) with the balance 25% N_2 or Ar (10 cm^3 min^{-1}) throughout the experiment. The tube was placed inside a furnace. Gas flows were controlled with Brooks 5850 mass flow controllers. Samples were first pre-treated by heating at 700 °C for 2 h in 75% H_2/N_2 to remove surface oxidation, then various temperatures and gas environments were applied as discussed later. Temperature changes were applied with a ramp rate of 5 °C min^{-1} and then maintained for 2 h, with the data used for refinement acquired toward the end of this period. Data were fitted using the GSAS package [33,34], using the structure model for Ni_2Mo_3N in $P4_132$ previously reported by Prior and Battle [35].

Results and Discussion

Ni_2Mo_3N adopts the filled β-manganese structure ($P4_132$), with corner-linked NMo_6 octahedra interpenetrated with a (10,3)-a network of nickel atoms (Fig. 1) [35]. Cobalt substitutes readily onto the Ni sites and the $(Ni,Co)_2Mo_3N$ system exhibited Vegard law behaviour (a linear variation in lattice parameter with composition) up to 50% cobalt [27], i.e. the $NiCoMo_3N$ composition also examined here. The coherent neutron scattering length of nitrogen (b_{coh} = 9.36 fm) is larger than that of most transition metals, and ~90% of that of nickel, the strongest scatterer in the Ni-Co-Mo-N system [36]. Hence PND is a very effective tool to examine the possibility of lattice nitrogen cycling and of a Mars-van Krevelen mechanism operating in ammonia synthesis [18,19]. Alongside examining any structure changes, isotopic exchange studies were also carried out to observe any lower level lattice nitrogen activity, providing sensitivity to exchange occurring only at surfaces where the diffraction study may be less sensitive.

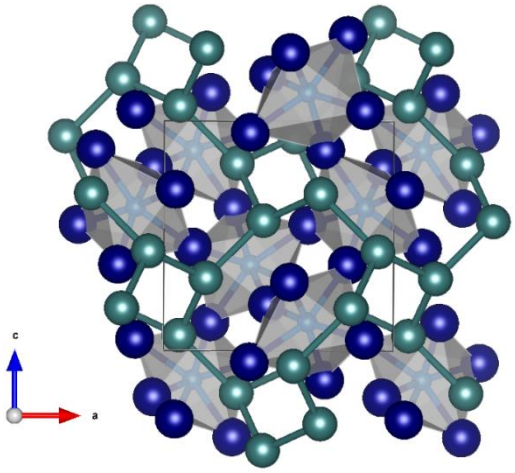

Figure 1. Structure of Ni_2Mo_3N viewed down [010], showing the corner linked NMo_6 (small blue N and large blue Mo) octahedra and the interpenetrating network of Ni (teal) atoms.

Catalytic activity of Ni_2Mo_3N and $NiCoMo_3N$ for ammonia synthesis

The catalytic activity of Ni_2Mo_3N and $NiCoMo_3N$ in ammonia synthesis was investigated using a 60 ml min^{-1} of 75% H_2:N_2 (BOC, H_2 99.998%, N_2 99.995%) gas mixture at 400 °C. The reaction conductivity profiles as function of time are presented in supplementary information (Fig. S1). Ammonia production yields were calculated from the reaction conductivity profiles as 116 μmol g^{-1} h^{-1} for Ni_2Mo_3N and 166 μmol g^{-1} h^{-1} for $NiCoMo_3N$. This compares with total nitrogen contents of the materials before catalysis of 2514 and 2314 μmol g^{-1} h^{-1} (respectively). As expected both Ni_2Mo_3N and $NiCoMo_3N$ have lower catalytic activities than some very active systems such as Co_3Mo_3N (652 μmol NH_3 g^{-1} h^{-1} [37]), which is known to have active lattice nitrogen, or CoRe (943 μmol NH_3 g^{-1} h^{-1} [38]) in similar conditions.

Figure 2 presents the XRD patterns collected on the as-prepared and post-reaction materials. The as-prepared materials had a phase-pure match to the filled β-manganese structure with space group $P4_132$. Post-reaction XRD analysis showed that the filled β-manganese structure was maintained upon reaction in both Ni_2Mo_3N and $CoNiMo_3N$. The evolution of the structural properties during ammonia synthesis reaction will be studied in more details using *in situ* PND in the following section.

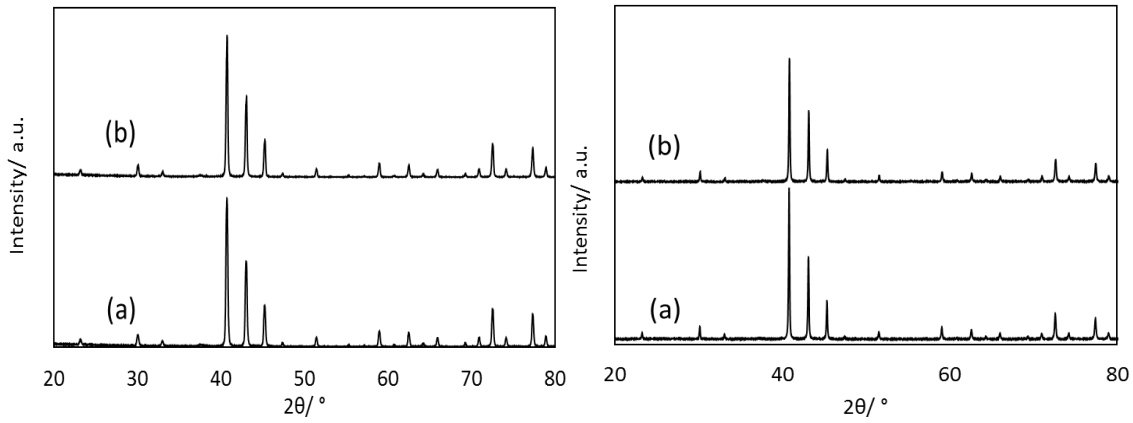

Figure 2. XRD patterns before (a) and after (b) catalytic reactions for Ni_2Mo_3N (left) and $NiCoMo_3N$ (right).

***In situ* powder neutron diffraction study**

During the *in situ* PND experiments samples were first pre-treated with an ammonia synthesis gas mix (75% H_2/N_2) for 2 h at 700 °C to remove the oxide passivation layer, then heating treatments in 75% H_2/N_2 or H_2/Ar were applied. If lattice nitrogen was active in ammonia synthesis it would be expected that the argon firing treatments would result in a reduction in the nitrogen occupancy, possibly with some associated structure transformation. The nitrogen treatments would retain the full nitrogen occupancy or produce a smaller reduction in the occupancy.

The PND data contained strong reflections due to the Ni_2Mo_3N (Fig. 3) or $NiCoMo_3N$, with a background due to the silica tube. Background subtraction using data from an empty silica tube was attempted, but due to variations in the tubes it was found to be more effective to simply fit the complex background shape, in which all features are much broader than the Bragg peaks of interest for the structure refinements. At ambient temperature it was found that the lattice parameter of $NiCoMo_3N$ was slightly larger than that of Ni_2Mo_3N, as expected from the larger ionic and metallic radii

of cobalt compared with nickel, and that the nitrogen occupancies of all samples were around 0.97±0.01 (Table 1).

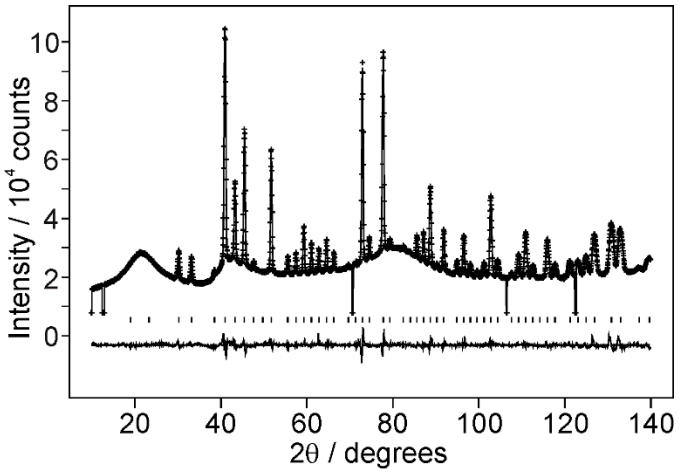

Figure 3. Fit to PND data for Ni_2Mo_3N at ambient temperature. Crosses mark the data points, the upper continuous line the fit, the lower continuous line the difference and tick marks the allowed reflection positions in $P4_132$. Full details of refined parameters are in supplementary information, Fig. S2a.

Table 1. Key parameters from *in situ* PND. In all cases samples were allowed to equilibrate at the given temperature for >1 h before the measurement was taken.

Run number and material	**Gas**	**T / °C**	***a* / Å**	**N site occupancy**	**Full details in SI**
1. Ni_2Mo_3N	H_2/N_2	Ambient	6.63050(9)	0.973(7)	Fig. S2a
	H_2/N_2	700	6.66794(10)	0.975(5)	Fig. S2b
	H_2/N_2	400	6.65045(10)	0.974(7)	Fig S2c
2. $NiCoMo_3N$	H_2/N_2	Ambient	6.63680(9)	0.966(6)	Fig. S3a
	H_2/N_2	700	6.67252(10)	0.949(5)	Fig. S3b
	H_2/N_2	400	6.65547(10)	0.959(5)	Fig. S3c
3. Ni_2Mo_3N	H_2/N_2	700	6.66484(13)	0.960(8)	Fig. S4a
	H_2/Ar	700	6.66454(13)	0.957(8)	Fig. S4b
	H_2/N_2	700	6.66494(13)	0.960(8)	Fig. S4c
4. $NiCoMo_3N$	H_2/N_2	Ambient	6.63655(9)	0.967(5)	Fig. S5a
	H_2/N_2	700	6.67326(11)	0.953(5)	Fig. S5b
	H_2/Ar	700	6.67268(11)	0.947(5)	Fig. S5c
	H_2/N_2	700	6.67332(10)	0.956(5)	Fig. S5d
5. Ni_2Mo_3N	H_2/N_2	Ambient	6.62841(10)	0.983(7)	Fig. S6a
	H_2/N_2	700	6.66509(11)	0.965(7)	Fig. S6b
	H_2/Ar	700	6.66465(11)	0.956(7)	Fig. S6c
	H_2/Ar	400	6.64725(10)	0.966(7)	Fig. S6d
	H_2/N_2	400	6.64761(10)	0.968(7)	Fig. S6e
6. $NiCoMo_3N$	H_2/N_2	Ambient	6.63574(10)	0.963(6)	Fig. S7a
	H_2/N_2	700	6.67554(12)	0.948(6)	Fig. S7b
	H_2/Ar	700	6.67496(11)	0.945(5)	Fig. S7c
	H_2/Ar	400	6.65567(10)	0.955(5)	Fig. S7d
	H_2/N_2	400	6.65634(10)	0.957(5)	Fig. S7e

The first heating conditions applied emulated ambient pressure ammonia synthesis conditions. The materials were simply heated under 75% H_2 / 25% N_2, first at 700 °C to activate the catalyst by removing surface oxide, then at 400 °C where ammonia synthesis is more favored due to a lower decomposition rate (Table 1, runs 1 and 2). The second investigated whether at the activation temperature nitrogen could be removed from the lattice by switching the gas to 75% H_2 / 25% Ar whilst at 700 °C, then back again (Table 2, runs 3 and 4). Finally, the samples were cooled from 700 to 400 °C in the H_2/Ar mix and then re-exposed to 75% H_2 / 25% N_2 to see whether the nitrogen content increased at the ammonia synthesis conditions (Table 2, runs 5 and 6). The striking finding is that the nitrogen occupancies do not change in a systematic manner within the resolution of the measurements and this is in stark contrast to the behavior of Co_3Mo_3N [18]. The average estimated standard deviation in the nitrogen occupancies is 0.007, and 3× esd is around 2% of the occupancies, so this suggests that any change which does occur is very small. Plotting the lattice parameters of samples under both gas environments against temperature (Fig. 4) also highlights that other than small sample to sample variations in the lattice parameter, the temperature is the factor that has the largest effect. Both materials show a fairly linear expansion over this temperature range of ~5.5×10^{-5} Å $°C^{-1}$.

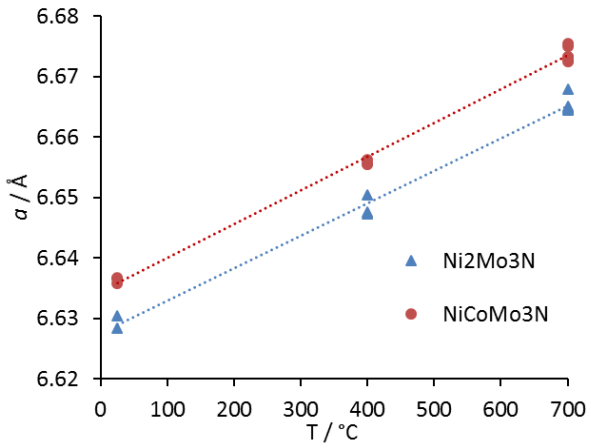

Figure 4. Lattice parameter variations with temperature in Ni_2Mo_3N and $NiCoMo_3N$ (all measured either in 75% H_2 / 25% N_2 or in 75% H_2 / 25% Ar.

Isotopic exchange studies

The ability of Ni_2Mo_3N and $NiCoMo_3N$ to activate molecular nitrogen was studied *via* temperature programmed nitrogen isotopic exchange (TPNIE). This involved heating the sample in a closed loop of $^{15}N_2$ in the range of 400 to 700 °C and monitoring the nitrogen isotopomers that were present by mass spectrometry. The results are presented in Fig. 5. Whilst small changes in the $^{15}N_2$ and $^{14}N_2$ concentrations were measured over time, critically the concentration of $^{15}N^{14}N$ does not rise. Hence any nitrogen exchange activity at the range of temperature studied is minimal, confirming that the high stability of the lattice nitrogen in the reaction conditions observed in the bulk by PND is representative of the sample as a whole.

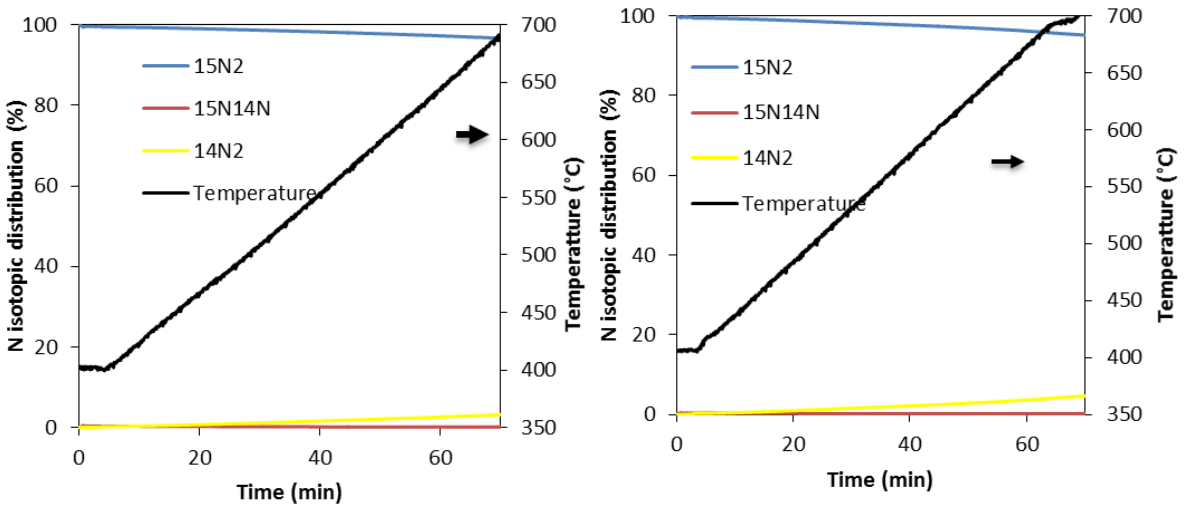

Figure 5. Evolution of the nitrogen isotopomer distribution during the heterolytic TPNIE experiment on Ni_2Mo_3N and $NiCoMo_3N$.

Conclusions

Structurally the metal and nitrogen coordination environments in the filled β-manganese structured Ni_2Mo_3N phase investigated herein are similar to those in Co_3Mo_3N. In order to investigate the relationship between structure type and lattice nitrogen activity, cobalt has been carefully introduced into Ni_2Mo_3N to move its electronic structure closer to that of Co_3Mo_3N. It has been found that the substitution of 50% of the Ni in the phase by Co has little effect upon lattice N reactivity. Lattice nitrogen reactivity does not seem to be able to be switched on by composition change, which is also in line with a recent study comparing Co_3Mo_3N with Co_2Mo_3N [28]. This suggests that structure type is more important than electronic aspects in this context. This may be linked to the stability of Co_6Mo_6N, which is formed on denitridation of Co_3Mo_3N with transfer of nitrogen to an alternative crystallographic site [19]. Investigation of the lattice reactivity in the, to date, unprecedented Ni_3Mo_3N phase [39] could prove informative. Activity in this phase space would also be a productive topic for a computational study.

Acknowledgements

The authors thank EPSRC for support under EP/J018384/1, EP/J019208/1 and EP/L02537X/1, the government of Saudi Arabia for a scholarship to SAS and the ILL for D20 beam time under award 5-23-671.

References

[1] J.S.J. Hargreaves, Nitrides as ammonia synthesis catalysts and as potential nitrogen transfer reagents, Appl. Petrochemical Res. 4 (2014) 3–10. doi:10.1007/s13203-014-0049-y.

[2] R. Michalsky, P.H. Pfromm, Chromium as reactant for solar thermochemical synthesis of ammonia from steam, nitrogen, and biomass at atmospheric pressure, Sol. Energy. 85 (2011) 2642–2654. doi:10.1016/j.solener.2011.08.005.

[3] R. Michalsky, B.J. Parman, V. Amanor-Boadu, P.H. Pfromm, Solar thermochemical production of ammonia from water, air and sunlight: Thermodynamic and economic analyses, Energy. 42

(2012) 251–260. doi:10.1016/j.energy.2012.03.062.

[4] R. Michalsky, P.H. Pfromm, Thermodynamics of Metal Reactants for Ammonia Synthesis from Steam, Nitrogen and Biomass at Atmospheric Pressure, AIChE J. 58 (2012) 3203–3213. doi:10.1002/aic.13717.

[5] R. Michalsky, P.H. Pfromm, An ionicity rationale to design solid phase metal nitride reactants for solar ammonia production, J. Phys. Chem. C. 116 (2012) 23243–23251. doi:10.1021/jp307382r.

[6] R. Michalsky, A.M. Avram, B.A. Peterson, P.H. Pfromm, A.A. Peterson, Chemical looping of metal nitride catalysts: Low-pressure ammonia synthesis for energy storage, Chem. Sci. 6 (2015) 3965–3974. doi:10.1039/c5sc00789e.

[7] R. Michalsky, P.H. Pfromm, A. Steinfeld, Rational design of metal nitride redox materials for solar-driven ammonia synthesis, Interface Focus. 5 (2015) 1–10. doi:10.1098/rsfs.2014.0084.

[8] N. Shan, V. Chikan, P. Pfromm, B. Liu, Fe and Ni Dopants Facilitating Ammonia Synthesis on Mn4N and Mechanistic Insights from First-Principles Methods, J. Phys. Chem. C. 122 (2018) 6109–6116. doi:10.1021/acs.jpcc.7b12569.

[9] J.M. McEnaney, A.R. Singh, J.A. Schwalbe, J. Kibsgaard, J.C. Lin, M. Cargnello, T.F. Jaramillo, J.K. Nørskov, Ammonia synthesis from N2 and H2O using a lithium cycling electrification strategy at atmospheric pressure, Energy Environ. Sci. 10 (2017) 1621–1630. doi:10.1039/c7ee01126a.

[10] G.E. Veitch, K.L. Bridgwood, S. V. Ley, Magnesium nitride as a convenient source of ammonia: Preparation of Primary Amides, Org. Lett. 10 (2008) 3623–3625. doi:10.1021/ol801398z.

[11] K.L. Bridgwood, G.E. Veitch, S. V. Ley, Magnesium nitride as a convenient source of ammonia: Preparation of Dihydropyridines, Org. Lett. 10 (2008) 3627–3629. doi:10.1021/ol801399w.

[12] S. Ley, Chemical safety Mg3N2 explosion risk, Chem. Eng. News. 87 (2009) 4–4.

[13] A.M. Alexander, J.S.J. Hargreaves, C. Mitchell, The reduction of various nitrides under hydrogen: Ni3N, Cu3N, Zn3N2 ad Ta3N5, Top. Catal. 55 (2012) 1046–1053. doi:10.1007/s11244-012-9890-3.

[14] S. Laassiri, C.D. Zeinalipour-Yazdi, C.R.A. Catlow, J.S.J. Hargreaves, Nitrogen transfer properties in tantalum nitride based materials, Catal. Today. 286 (2017) 147–154. doi:10.1016/j.cattod.2016.06.035.

[15] A.M. Alexander, J.S.J. Hargreaves, C. Mitchell, The denitridation of nitrides of iron, cobalt and rhenium under hydrogen, Top. Catal. 56 (2013) 1963–1969. doi:10.1007/s11244-013-0133-z.

[16] S. Laassiri, C.D. Zeinalipour-Yazdi, C.R.A. Catlow, J.S.J. Hargreaves, The potential of manganese nitride based materials as nitrogen transfer reagents for nitrogen chemical looping, Appl. Catal. B Environ. 223 (2018) 60–66. doi:10.1016/j.apcatb.2017.04.073.

[17] C.D. Zeinalipour-Yazdi, J.S.J. Hargreaves, S. Laassiri, C.R.A. Catlow, DFT-D3 study of H2 and N2 chemisorption over cobalt promoted Ta3N5 -(100), (010) and (001) surfaces, Phys. Chem. Chem. Phys. 19 (2017) 11968–11974. doi:10.1039/C7CP00806F.

[18] D. Mckay, D.H. Gregory, J.S.J. Hargreaves, S.M. Hunter, X. Sun, Towards nitrogen transfer catalysis: Reactive lattice nitrogen in cobalt molybdenum nitride, Chem. Commun. 7 (2007)

3051–3053. doi:10.1039/b707913c.

[19] S.M. Hunter, D. McKay, R.I. Smith, J.S.J. Hargreaves, D.H. Gregory, Topotactic nitrogen transfer: Structural transformation in cobalt molybdenum nitrides, Chem. Mater. 22 (2010) 2898–2907. doi:10.1021/cm100208a.

[20] D.H. Gregory, J.S.J. Hargreaves, S.M. Hunter, On the regeneration of Co3Mo3N from Co6Mo6N with N2, Catal. Letters. 141 (2011) 22–26. doi:10.1007/s10562-010-0464-3.

[21] S.M. Hunter, D.H. Gregory, J.S.J. Hargreaves, M. Richard, D. Duprez, N. Bion, A study of 15N/14N isotopic exchange over cobalt molybdenum nitrides, ACS Catal. 3 (2013) 1719–1725. doi:10.1021/cs400336z.

[22] C.D. Zeinalipour-Yazdi, J.S.J. Hargreaves, C.R.A. Catlow, Nitrogen Activation in a Mars-van Krevelen Mechanism for Ammonia Synthesis on Co3Mo3N, J. Phys. Chem. C. 119 (2015) 28368–28376. doi:10.1021/acs.jpcc.5b06811.

[23] C.D. Zeinalipour-Yazdi, J.S.J. Hargreaves, C.R.A. Catlow, DFT-D3 Study of Molecular N2 and H2 Activation on Co3Mo3N Surfaces, J. Phys. Chem. C. 120 (2016) 21390–21398. doi:10.1021/acs.jpcc.6b04748.

[24] C.D. Zeinalipour-Yazdi, J.S.J. Hargreaves, C.R.A. Catlow, Low-T Mechanisms of Ammonia Synthesis on Co3Mo3N, J. Phys. Chem. C. 122 (2018) 6078–6082. doi:10.1021/acs.jpcc.7b12364.

[25] D. Mckay, J.S.J. Hargreaves, J.L. Rico, J.L. Rivera, X.L. Sun, The influence of phase and morphology of molybdenum nitrides on ammonia synthesis activity and reduction characteristics, J. Solid State Chem. 181 (2008) 325–333. doi:10.1016/j.jssc.2007.12.001.

[26] S.M. Hunter, PhD thesis: Molybdenum Nitrides: Structural and Reactivity Studies, University of Glasgow, 2012.

[27] N. Bion, F. Can, J. Cook, J.S.J. Hargreaves, A.L. Hector, W. Levason, A.R. McFarlane, M. Richard, K. Sardar, The role of preparation route upon the ambient pressure ammonia synthesis activity of Ni2Mo3N, Appl. Catal. A Gen. 504 (2015) 44–50. doi:10.1016/j.apcata.2014.10.030.

[28] P. Adamski, D. Moszyński, M. Nadziejko, A. Komorowska, A. Sarnecki, Thermal stability of catalyst for ammonia synthesis based on cobalt molybdenum nitrides, Chem. Pap. 73 (2019) 851–859. doi:10.1007/s11696-018-0642-0.

[29] Y. Abghoui, A.L. Garden, J.G. Howalt, T. Vegge, E. Skúlason, Electroreduction of N2 to Ammonia at Ambient Conditions on Mononitrides of Zr, Nb, Cr, and V: A DFT Guide for Experiments, ACS Catal. 6 (2016) 635–646. doi:10.1021/acscatal.5b01918.

[30] Y. Abghoui, E. Skúlason, Computational Predictions of Catalytic Activity of Zincblende (110) Surfaces of Metal Nitrides for Electrochemical Ammonia Synthesis, J. Phys. Chem. C. 121 (2017) 6141–6151. doi:10.1021/acs.jpcc.7b00196.

[31] Y. Abghoui, E. Skúlason, Onset potentials for different reaction mechanisms of nitrogen activation to ammonia on transition metal nitride electro-catalysts, Catal. Today. 286 (2017) 69–77. doi:10.1016/j.cattod.2016.11.047.

[32] Y. Abghoui, E. Skúlason, Electrochemical synthesis of ammonia via Mars-van Krevelen mechanism on the (111) facets of group III–VII transition metal mononitrides, Catal. Today.

286 (2017) 78–84. doi:10.1016/j.cattod.2016.06.009.

[33] A.C. Larson, R.B. Von Dreele, General Structure Analysis System (GSAS), Regents Univ. Calif. 748 (1985) LAUR 86-748.

[34] B.H. Toby, EXPGUI, a graphical user interface for GSAS, J. Appl. Crystallogr. 34 (2001) 210–213. doi:10.1107/S0021889801002242.

[35] T.J. Prior, P.D. Battle, Facile synthesis of interstitial metal nitrides with the filled β - manganese structure, J. Solid State Chem. 172 (2003) 138–147. doi:10.1016/S0022-4596(02)00171-8.

[36] V. Sears, Neutron Scattering Lengths and Cross Sections, Nuetron News. 3 (1992) 26–37. doi:10.1080/10448639208218770.

[37] R. Kojima, K.-I. Aika, Cobalt molybdenum bimetallic catalysts for ammonia synthesis: Part 1. Preparation and Characterisation., Appl. Catal. A Gen. 215 (2001) 149–160. doi:10.1016/S0926-860X(01)00529-4.

[38] K. McAulay, J.S.J. Hargreaves, A.R. McFarlane, D.J. Price, N.A. Spencer, N. Bion, F. Can, M. Richard, H.F. Greer, W.F. Zhou, The influence of pre-treatment gas mixture upon the ammonia synthesis activity of Co–Re catalysts, Catal. Commun. 68 (2015) 53–57. doi:10.1016/j.catcom.2015.04.016.

[39] J.O. Conway, T.J. Prior, Interstitial nitrides revisited - a simple synthesis of MxMo3N (M = Fe, Co, Ni), J. Alloys Compd. 774 (2019) 69–74. doi:10.1016/j.jallcom.2018.09.307.